Archives of Biochemistry and Biophysics 485 (2009) 102–108

Contents lists available at ScienceDirect

Archives of Biochemistry and Biophysics

journal homepage: www.elsevier.com/locate/yabbi

Characterization of the ATPase activity of a novel chimeric fusion protein consisting of the two nucleotide binding domains of MRP1

Lixin Wan [a,b], Xingjie Liang [c], Youguo Huang [a,*]

[a] National Laboratory of Biomacromolecules, Center for structural and Molecular Biology, Institute of Biophysics, Chinese Academy of Sciences, 15 Datun Road, Beijing 100101, PR China
[b] Graduate School of the Chinese Academy of Sciences, Bejing 100049, PR China
[c] Laboratory of Nanobiomedicine and Nanosafety, Division of Nanomedicine and Nanobiology, National Center for Nanosciences and Technology of China, Beijing 100190, PR China

ARTICLE INFO

Article history:
Received 9 December 2008
and in revised form 28 February 2009
Available online 11 March 2009

Keywords:
MRP1
Multidrug resistance
Nucleotide binding domains
Domain–domain interaction
ATPase activity
Conformation

ABSTRACT

Nucleotide Binding Domains (NBDs) are responsible for the ATPase activity of the multidrug resistance protein 1 (MRP1). A series of NBD1-linker-NBD2 chimeric fusion proteins were constructed, expressed and purified, and their ATPase activities were analyzed. We report here that a GST linked $NBD1_{642-890}$-GST-$NBD2_{1286-1531}$ was able to hydrolyze ATP at a rate of about 4.6 nmol/mg/min (K_m = 2.17 mM, V_{max} = 12.36 nmol/mg/min), which was comparable to the purified and reconstituted MRP1. In contrast, neither a mixture of NBD1 and GST-NBD2 nor the NBD1-GST-NBD1 fusion protein showed detectable ATPase activity. Additionally, the E1455Q mutant was found to be nonfunctional. Measurements by both MIANS labeling and circular dichroism spectroscopy revealed significant conformational differences in the NBD1-GST-NBD2 chimeric fusion protein compared to the mixture of NBD1 and GST-NBD2. The results suggest a direct interaction mediated by GST between the two NBDs of MRP1 leading to conformational changes which would enhance its ATPase activity.

Introduction

The Multi-drug Resistance Protein 1 (MRP1/ABCC1) contains two nucleotide binding domains, NBD1 and NBD2, which through their interaction are responsible for the ATPase activity of the protein [1]. Like other ABC type ATPases, MRP1 utilizes the NBD-NBD interaction to bind and hydrolyze ATP, which provides the power stroke for the substrate transport. The inter-domain dimerization of two NBDs is facilitated by subtle regulation from other moieties of the intact molecule or protein complex, such as transmembrane domains [2] or other regulatory domains [3]. The dimerized NBDs bind two molecules of ATP at their interface, the so-called ATP binding pocket. The binding pocket is formed by side chains of amino acids from conserved motifs of both NBDs, including the Walker A, the Q-loop, and the stacked aromatic residues from one NBD and the ABC signature motif from the opposite NBD [4]. However, the dimerized state of the two NBDs is transient [5], which makes structural determination of the isolated NBD dimer very difficult.

Purified and reconstituted MRP1 displays relatively low ATPase activity, with a V_{max} of 5–10 nmol/mg/min (about 16–32 × 10^{-3} s^{-1}) [6,7], which is much lower than that of the P-glycoprotein (P-gp) (4.5–6.5 μmol/mg/min) [8]. However, the K_m value of MRP1 for ATP (100–300 μM) is comparable with that of P-gp (600 μM). Owing to its lower ATPase activity, the ATPase activity of MRP1 is difficult to measure using crude membrane. It is also difficult to purify and reconstitute MRP1, which is a large (~190 kDa) integral membrane protein. Therefore, to be able to study the regulatory role of inter-domain interactions in the catalytic cycle, it is necessary to express only the soluble nucleotide binding domains of MRP1.

Isolated NBD1 and NBD2 of MRP1 were cloned and purified by Ramaen et al., and it was found that individually, both NBDs displayed extremely low ATPase activities (0.02 nmol/mg/min [10^{-5} s^{-1}] and 0.01 nmol/mg/min [6×10^{-6} s^{-1}] for NBD1 and NBD2, respectively). Moreover, there were no indications that mixing NBD1 and NBD2 increased the ATPase activity or resulted in a stable interaction between the domains [9,10]. Structural determination of NBD1 by Ramaen et al. revealed a non-productive conformation at its catalytic site [11]. This result may imply that the productive interaction between NBD1 and NBD2 exists only within the intact protein, and is probably mediated by other segments of the molecule. It should also be noticed that some ABC proteins take advantage of additional peptides as linkers to stabilize two NBDs, as in the cases of MalK [3] and RLI [12].

In order to investigate the interaction between NBD1 and NBD2 of MRP1, we have attempted to use peptide linkers to connect two NBDs into NBD1-linker-NBD2 constructs which were subsequently expressed as chimeric fusion proteins. After purification, ATPase activities of the chimeric proteins were determined. Our results

* Corresponding author. Fax: +86 10 64888518.
E-mail address: huang@sun5.ibp.ac.cn (Y. Huang).

0003-9861/$ - see front matter © 2009 Elsevier Inc. All rights reserved.
doi:10.1016/j.abb.2009.03.003

suggest that the interaction between the NBDs of MRP1 required for its ATPase activity may be facilitated by certain linkers (e.g. GST).

Materials and methods

Construction of recombinant NBDs expression vectors

The cDNA fragments corresponding to NBD1 and NBD2 were amplified by PCR from pNUT-MRP1/His, a gift from Dr. Xiu-bao Chang [13]. In order to generate pET21a-MRP1-NBD1$_{642-871}$, the forward primer 5′-TAG CAT ATG AAC AGC ATC ACC GTG-3′ and the reverse primer 5′-TAG AAG CTT GCT GGC ATA GGT AC-3′ were used, and the NBD1 cDNA was cloned into pET21a (Novagen) as a NdeI-HindIII fragment. To generate pET30a-MRP1-NBD2$_{1286-1531}$, the forward primer 5′-TAG GGA TCC AGC TGG CCC CAG GTG-3′ and the reverse primer 5′-TAG AAG CTT TCA CAC CAA GCC GGC GTC-3′ were used, and the NBD2 cDNA was cloned into pET30a (Novagen) as a BamHI–HindIII fragment. To generate pGEX-6P-1-NBD2$_{1286-1531}$, the forward primer 5′-TAG GGA TCC AGC TGG CCC CAG GTG-3′ and the reverse primer 5′-TAG CTC GAG TCA CAC CAA GCC GGC GTC-3′ were used, the NBD2 cDNA was cloned into pGEX-6P-1 (Amersham) as a BamHI–XhoI fragment. To construct pET21a-NBD1$_{642-890}$-GST-NBD2$_{1286-1531}$, the NBD1$_{642-890}$ fragment was amplified using primers 5′-TAG GCT AGC AAC AGC ATC ACC GTG AG-3′ and 5′-TA GGT ACC CCC TGG ACC GCT GAC-3′, while the GST-NBD2$_{1286-1531}$ fragment was amplified from pGEX-6P-1-NBD2$_{1286-1531}$, using primers 5′-TAG GGT ACC TCC CCT ATA CTA GGT TAT TG-3′ and 5′-TAG AAG CTT CAC CAA GCC GGC GTC-3′, the NheI–KpnI fragment containing NBD1 and the KpnI–HindIII fragment containing GST-NBD2 were ligated together into pET21a. In order to introduce the E1455Q mutation into NBD2 of the pET21a-NBD1-GST-NBD2 construct, primers 5′-GAA GAT CCT TGT GTT GGA TCA GGC CAC GGC AGC CGT GGA CCT GG-3′ and 5′-CCA GGT CCA CGG CTG CCG TGG CCT GAT CCA ACA CAA GGA TCT TC-3' were used, and pET21a-NBD1-GST-NBD2 construct was used as template in the mutagenesis using QuikChange site directed mutagenesis kit (Stratagene). All constructs were verified by sequencing.

Overexpression and protein purification

Escherichia coli Rosetta(DE3) competent cells (Novagen) were transformed with the recombinant NBDs expression vectors and grown at 37 °C in 2YT medium containing ampicillin (100 μg/ml, for NBD1/6His, GST-NBD2 and NBD1-GST-NBD2/6His expression) or kanamycin (50 μg/ml, for NBD2/6His expression) until the absorbance at 600 nm reached a value of 0.6. Gene expression was induced with 0.1 mM IPTG (isopropyl-1-thio-β-D-galactopyranoside, Sigma) for 20 h at 16 °C and cells were harvested by centrifugation (4000*g* for 30 min) at 4 °C. All purification steps were performed at 4 °C.

For the NBD1/6His and NBD2/6His purification, cell pellet was resuspended in buffer A (25 mM Tris–HCl pH 8.0, 500 mM NaCl, 2 mM $MgCl_2$, 10 mM imidazole, 1 mM PMSF, 1 mM 2-mercaptoethanol). The cells were lysed by sonication (4 s on/8 s off, 200 cycles) in a cell sonicator (Cole-Parmer) and centrifuged at 20,000*g* for 40 min to precipitate the insoluble fraction of the cell extract. The supernatant was applied onto a 2 mL Ni-NTA His•Bind resin (Novagen) column equilibrated with buffer A. After washing with 20 column volumes of buffer A with 10 mM imidazole, the proteins were eluted with buffer B (25 mM Tris–HCl pH 8.0, 500 mM NaCl, 2 mM $MgCl_2$, 250 mM imidazole, 1 mM DTT, 10% glycerol). The eluted fractions were collected and concentrated with an Amicon Ultra-4 centrifugal filter unit (Millipore) to a final volume of 500 μL. The concentrated proteins were loaded onto a Superdex 200 HR 10/30 gel filtration column (Amersham) equilibrated with buffer C (25 mM Tris–HCl pH 8.0, 150 mM NaCl, 2 mM $MgCl_2$, 1 mM DTT), elution profile was monitored at 280 nm using a flow rate of 0.3 ml/min, fractions were analyzed by SDS–PAGE. Proteins were concentrated to 10–20 mg/mL and stored at −80 °C in buffer C containing 10% glycerol. Protein concentration was determined with the BCA protein assay kit (Pierce).

For GST-NBD2 purification, cell pellet was resuspended in buffer D (144 mM NaCl, 2.7 mM KCl, 10 mM Na_2HPO_4, 1.8 mM KH_2PO_4, 1 mM PMSF, pH 7.3). The cells were lysed by sonication (4 s on/8 s off, 200 cycles) in a cell sonicator (Cole-Parmer) and centrifuged at 20,000*g* for 40 min to precipitate the insoluble fraction of the cell extract. The supernatant was applied onto a 2 mL Glutathione Sepharose 4B resin (Amersham) column equilibrated with buffer D. After washing with 20 column volumes of buffer D, the proteins were eluted with buffer E (50 mM Tris–HCl, 150 mM NaCl, 2 mM $MgCl_2$, 1 mM DTT, 10 mM reduced glutathione, pH 8.0). The eluted fractions were collected, concentrated, and further purified by Superdex 200 gel filtration column as described above.

For the NBD1-GST-NBD2/6His (designated as NBD1-GST-NBD2 below) purification, collected cell pellet was first lysed and purified using Ni–NTA His•Bind column as described above. Proteins eluted from Ni–NTA His•Bind column were dialysed against buffer D containing 1 mM DTT. The dialysed sample was applied to Glutathione Sepharose 4B column as described in GST-NBD2 purification above with exceptions that the flow rate was limited to 0.2 mL/min and the flow-through was reloaded onto the column for 3 times to ensure effective binding. Eluted protein sample was concentrated, and further purified by Superdex 200 gel filtration column as described above.

Purified NBDs proteins were analyzed by SDS–PAGE and immunoblot using anti-MRP1 NBD1 monoclonal antibody 42.4 or anti-MRP1 NBD2 monoclonal antibody 897.2, both gifts from Dr. Xiu-bao Chang [14].

ATPase activity

The ATPase activity of MRP1 was determined as described previously [15] by using a colorimetric method to measure the release of inorganic phosphate from ATP. Typically, 10–20 μg of the purified protein was incubated at 37 °C in 0.1 ml assay buffer containing 50 mM Tris–HCl, pH 7.4, 2 mM ATP, 2 mM $MgCl_2$ for 200 min.

Protease cleavage

Purified protein (10 μg) was cleaved by 5 μg ProScission protease (Amersham) in a buffer containing 50 mM Tris–HCl, 100 mM NaCl for 8 h at 4 °C. The cleaved samples were applied to SDS–PAGE (10% gel) and immunoblotted using anti-MRP1 NBD1 monoclonal antibody 42.4 or anti-MRP1 NBD2 monoclonal antibody 897.2.

MIANS labeling

MIANS (2-(4-maleimidoanilino) naphthalene-6-sulfonic acid, Molecular Probes) solution was prepared as previously described [16]. To fully label the recombinant proteins with MIANS, 0.1 μM of each protein was incubated with 2 μM MIANS at 22 °C for 1 h in a buffer containing 50 mM Tris–HCl pH 7.5, 100 mM NaCl, 2 mM $MgCl_2$, and the fluorescence spectra of covalently bound MIANS were measured with $\lambda_{ex} = 322$ nm, using free MIANS to generate a standard curve, and the unlabeled proteins as a blank.

Circular dichroism (CD) spectroscopy

The CD spectra for the purified recombinant proteins were recorded between 200 and 250 nm at 24 °C in a 1 mm path cuvette

using a Jasco J720 spectropolarimeter. Proteins were diluted in a buffer containing 50 mM Tris–HCl pH 7.5, 100 mM NaCl, 2 mM $MgCl_2$ at concentration of 3.33 μM.

Results

Design of the recombinant NBD1-linker-NBD2 chimeric fusion proteins

Six different peptide linkers were selected to construct NBD1-linker-NBD2 chimeric proteins (Fig. 1). Some of these had previously been used as artificial peptide linkers to study protein–protein interactions [17], including the helical linkers $(EAAAR)_2$ and $(EAAAR)_4$, and the flexible linkers $(G_4S)_2$ and $(G_4S)_4$. The RLI Hinge I peptide was chosen from a *Pyrococcus furiosus* ABC ATPase RNase-L inhibitor which is composed of 42 amino acids (Gln^{295} to Arg^{336}). RLI Hinge I has been suggested to function as a joint between two NBDs of RLI to allow ATP-driven conformational changes in the NBDs [12]. The *Schistosoma japonicum* Glutathione S-transferase (GST) protein containing amino acids S^2 to D^{220} was obtained from pGEX-6p-1 vector. The selected amino acid ranges for NBD1 and NBD2 were basically the same as those used by Ramaen et. al. [9,10], encompassing Asn^{642}-Ser^{871} for NBD1 and Ser^{1286}-Val^{1531} for NBD2, respectively. However, we also made adjustments to the C-terminal of NBD1 and the N-terminal of NBD2 to obtain more soluble expression. For instance, extension of the C-terminal of NBD1 to Gly^{890}, yielding a longer flexible region between NBD1 and the peptide linker, increased the soluble expression of the fusion protein.

Identification of purified recombinant NBDs proteins by SDS–PAGE and immunoblot

NBD1 with a C-terminal 6His-tag was overexpressed in *E. coli* and purified as a soluble fusion protein (theoretical molecular mass 26.4 kDa). The NBD1 fractions obtained from chelating affinity chromatography and subsequent gel filtration chromatography both produced single bands SDS–PAGE analysis (Fig. 2A L1, L2). The elution profile of NBD1 on a Superdex 200 column was also overwhelming monomer (data not shown), with an apparent molecular mass of less than 30 kDa. Purification of NBD2 with a N-terminal 6His-tag (theoretical molecular mass of 33.1 kDa) displayed a similar profile (Fig. 2A L3, L4), with exceptions that the yield of NBD2 was much smaller than that of NBD1, and that NBD2 eluted from Superdex 200 column contained about 40% oligomers (data not shown). Attempts to express NBD2 as an NdeI–HindIII fragment with a C-terminal 6His-tag in pET21a did not yield any inducible expression. Insertion of NBD2 into pET21a as a BamHI–HindIII fragment, produced a fusion protein with a short T7 tag at its N-terminal, whose induced expression was found in inclusion bodies, and hardly any soluble expression could be obtained even at low concentration of IPTG (0.1 mM) and low temperature (16 °C). Only when expressed with a longer N-terminal fusion peptide, as in pET30a, could NBD2 be expressed as soluble protein. In contrast to NBD2, GST-NBD2 was first purified using glutathione affinity chromatography, and the eluted protein migrated in SDS–PAGE as a band of about 55 kDa (Fig. 2A L5, L6), coincident with its theoretical molecular mass of 55.2 kDa. The majority of eluted GST-NBD2 from Superdex 200 column formed a dimer (data not shown), caused by the dimerization of the GST moiety of the fusion protein.

A three-step procedure was used for NBD1-GST-NBD2 purification as described in Materials and methods. By taking advantage of its C-terminal 6His-tag and its GST domain, the fusion protein was purified using distinct and sequential affinity chromatographic steps, followed by a polishing gel filtration purification step. NBD1-GST-NBD2 was first purified using chelating affinity chromatography, which resulted in the eluted proteins with a relative low purity as analyzed by SDS–PAGE (Fig. 2A L7). The proteins were thereafter applied to glutathione affinity chromatography, however, the efficiency of NBD1-GST-NBD2 binding to glutathione sepharose resin was quite low, and circular sample loading was used to accomplish better binding. SDS–PAGE analysis of the eluate from glutathione sepharose resin revealed a substantial improvement in protein purity (Fig. 2A L8). A gel filtration chromatographic profile of the

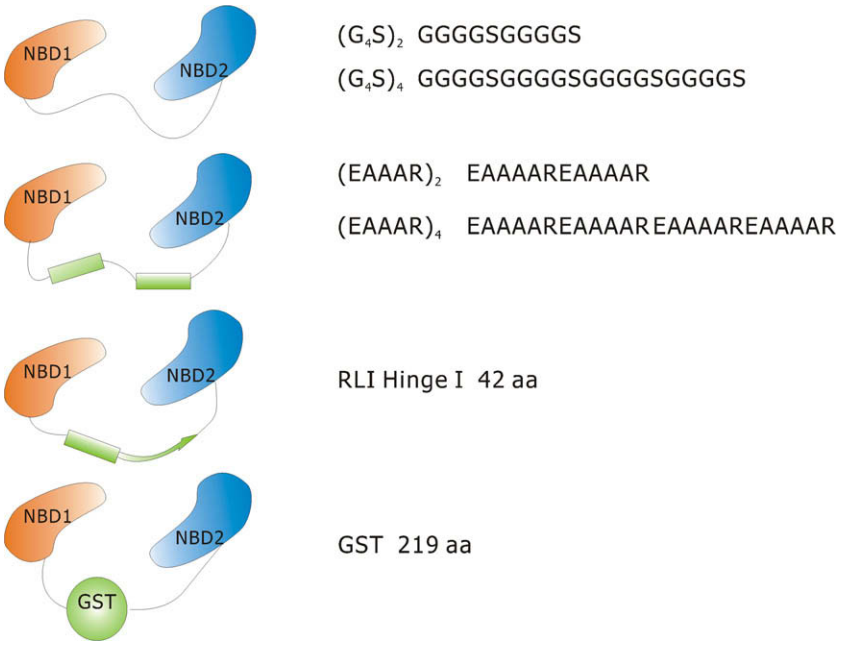

Figure 1. Construction of NBD1-linker-NBD2 chimeric proteins. The figures show the different types of linkers used to connect the NBD1 and NBD2 domains, including their amino acid sequences. $(G_4S)_2$, $(G_4S)_4$, $(EAAAR)_2$ and $(EAAAR)_4$ are short artificial peptide linkers that possess either flexible or helical conformation. RLI Hinge I is a linker region ranging from Gln^{295} to Arg^{336} in the *Pyrococcus furiosus* ABC ATPase RNase-L inhibitor. The *Schistosoma japonicum* Glutathione S-transferase (GST) protein is composed of 219 amino acids ranging from S^2 to D^{220}.

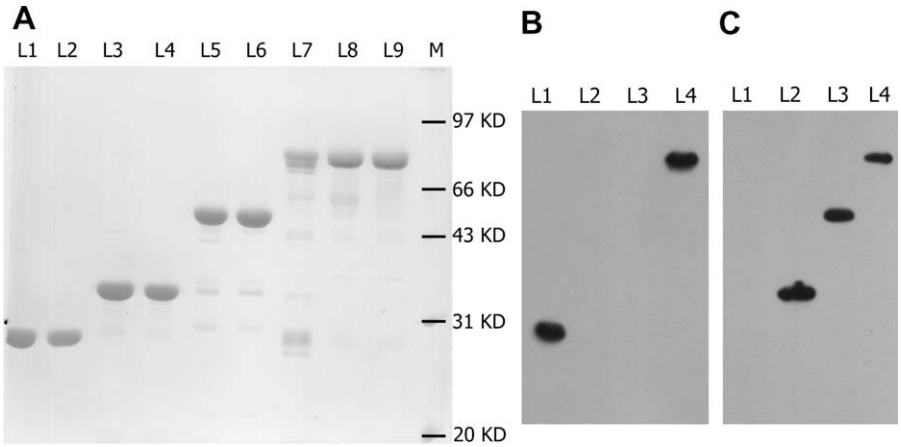

Figure 2. Purification of NBD1, NBD2, GST-NBD2, and NBD1-GST-NBD2. The NBD1, NBD2, GST-NBD2 and NBD1-GST-NBD2 proteins were purified as described in the Materials and methods section, the eluted proteins were analysed by SDS–PAGE (12% gel), and then detected using Coomassie Blue staining or subjected to immunoblot. (A) SDS–PAGE analysis of the purified proteins, 2 μg protein was loaded in each lane: L1 and L2, NBD1 purified on His•bind resin and Superdex 200 respectively; L3 and L4, NBD2 purified on His•bind resin and Superdex 200 respectively; L5 and L6, GST-NBD2 purified on glutathione sepharose resin and Superdex 200 respectively; L7, L8 and L9, NBD1-GST-NBD2 purified on His•bind resin, on glutathione sepharose resin and Superdex 200 respectively. (B and C) Immunoblot analysis of Superdex 200 purified proteins by either anti-NBD1 mAb 42.4 (B) or anti-NBD2 mAb 897.2 (C). L1: NBD1, L2: NBD2, L3: GST-NBD2, L4: NBD1-GST-NBD2.

protein further suggested that a major fraction of the NBD1-GST-NBD2 existed in the form of a dimer, along with a few oligomers (data not shown). The final protein yield of NBD1-GST-NBD2 was nonetheless quite low, with about 100–200 μg per liter culture, compared with about 5–20 mg for single NBDs, and 1–2 mg for short NBD1-linker-NBD2 peptides. To increase expression we therefore attempted a number of changes in amino acid sequence of both the C-terminal of NBD1 and the N-terminal of NBD2, and eventually observed that a short extension of the NBD1 C-terminal to G_{890} rather than to S_{871} moderately increased the protein yield. The apparent molecular mass of $NBD1_{642-890}$-GST-$NBD2_{1286-1531}$ as observed in both SDS–PAGE and gel filtration chromatography (as a dimer) was coincident with the theoretical 82.5 kDa molecular mass of the molecule. Purified NBD1, NBD2, GST-NBD2 and NBD1-GST-NBD2 were also subjected to immunoblot analysis using either anti-MRP1 NBD1 mAb 42.4 or anti-MRP1 NBD2 mAb 897.2. The results indicated immunoreactivity of NBD1 and NBD1-GST-NBD2 to mAb 42.4, while NBD2, GST-NBD2 and NBD1-GST-NBD2 indicated immunoreactivity to mAb 897.2 (Fig. 2B and C).

Purity of the NBD1-GST-NBD2 chimeric fusion protein determined by PreScission protease

To further assess the purity of NBD1-GST-NBD2, we utilized PreScission protease to specifically cleave the fusion protein into NBD1-GST and NBD2. After cleavage at 4 °C for 8 h, the reaction mixture was analyzed by SDS–PAGE and immunoblot. As shown in Fig. 3, purified NBD1-GST-NBD2 was completely cleaved by protease, in contrast, proteins eluted from His•Bind resin was not significantly cleaved. This result was further confirmed by Western blot assay (Fig. 3B) indicating an accurate location of the cleaveage site between NBD1-GST and NBD2.

The NBD1-GST-NBD2 chimeric fusion protein shows ATPase activity

We assayed the ATPase activity of the various NBD1-linker-NBD2 chimeric fusion proteins constructed with the six different peptide linkers. As shown in Fig. 4A, the four fusion proteins formed with short peptide linkers (e.g., NBD1-$(G_4S)_4$-NBD2) showed no detectable ATPase activity after purification on a Superdex 200 gel filtration column. In addition, although different strategies used for their purification of NBD1, NBD2 and GST-NBD2, they all lost the capability to hydrolyze ATP after the gel filtration step (Fig. 4A). Nor did a mixture of NBD1 with either NBD2 or GST-NBD2 (designated as NBD1(+)NBD2 or NBD1(+)GST-NBD2 below) show any detectable ATPase activity (Fig. 4B). These findings are all consistent with previous reports [10]. On the other hand, the fusion proteins formed with the two longer peptides linker did show ATPase activity even after the gel filtration step. The NBD1-HingeI-NBD2 fusion protein (linked by RLI Hinge I) was able to hydrolyze ATP at a quite low rate of 0.56 nmol/mg/min (5.36×10^{-4} s^{-1}; Fig. 4A), whereas the GST linked fusion protein NBD1-GST-NBD2 produced an ATPase activity of about 4.6 nmol/mg/min (6.34×10^{-3} s^{-1}; Fig. 4A). To evaluate the enzymic parameters, the ATP hydrolytic activity of the NBD1-GST-NBD2 protein was measured as a function of the ATP concentration. Michaelis–Menten curves were determined, yielding V_{max} and K_m values of 12.36 nmol/mg/min (17.0×10^{-3} s^{-1}) and 2.17 mM, respectively (Fig. 4C and D). Thus, the purified NBD1-GST-NBD2 showed a maximal velocity of ATP hydrolysis comparable to that of the intact MRP1 (5–10 nmol/mg/min, or $16–32 \times 10^{-3}$ s^{-1}), but a several fold lower affinity for ATP than the intact MRP1 (100–300 μM).

To further confirm the ATPase activity of the chimeric fusion protein NBD1-GST-NBD2, domain replacement and site-directed mutagenesis of the fusion protein were performed. To this end, we constructed a NBD1-GST-NBD1 fusion protein and an E1455Q mutant of the NBD1-GST-NBD2 fusion protein. Both were expressed and purified in the same way as for NBD1-GST-NBD2. Similar to isolated NBD1 and NBD2, neither NBD1-GST-NBD1 nor NBD1-GST-NBD2/E1455Q showed any detectable ATPase activity (Fig. 4B). These results indicated that the ATPase activity of the NBD1-GST-NBD2 chimeric fusion protein is intrinsic rather than arising from contamination, and that its ATPase activity level is comparable to that of the intact MRP1.

The NBD1-GST-NBD2 chimeric fusion protein has specific conformational characteristics

MIANS, a fluorescent probe sensitive to changes in the microenvironment polarity of a protein molecule, has been used to study conformational changes in the P-gp [16] and MRP1 [18] proteins. MIANS only shows fluorescence after its maleimide moiety has undergone a covalent reaction with sulfhydryl groups. This feature allows specific labeling of accessible cysteine residues on a protein,

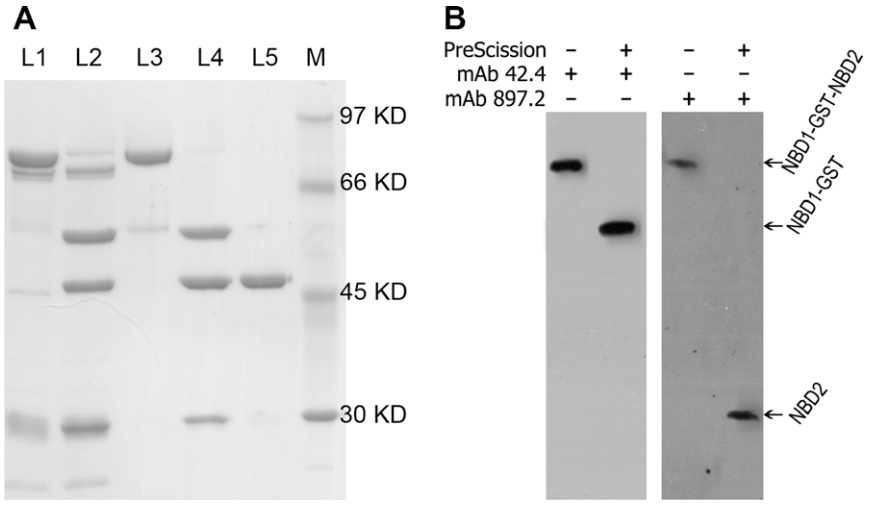

Figure 3. PreScission cleavage of chimeric fusion protein NBD1-GST-NBD2. Purified NBD1-GST-NBD2 (10 μg) from His•bind resin and Superdex 200 column was cleaved by 5 μg protease in buffer containing 50 mM Tris–HCl, 100 mM NaCl for 8 h at 4 °C. Cleaved sample containing 2 μg protein was applied to SDS–PAGE (10% gel) and 0.02 μg protein was applied to immunoblot using anti-MRP1 NBD1 mAb 42.4 or anti-MRP1 NBD2 mAb 897.2. (A) SDS–PAGE of NBD1-GST-NBD2 cleavage. Lane 1 and 2, protein purified on His•bind resin before and after PreScission cleavage; Lane 3 and 4, protein purified from Superdex 200 column before and after PreScission cleavage; Lane 5, 2 μg PreScission. M, molecular-mass standards. (B) Immunoblot of NBD1-GST-NBD2 purified from Superdex 200 column before and after PreScission cleavage.

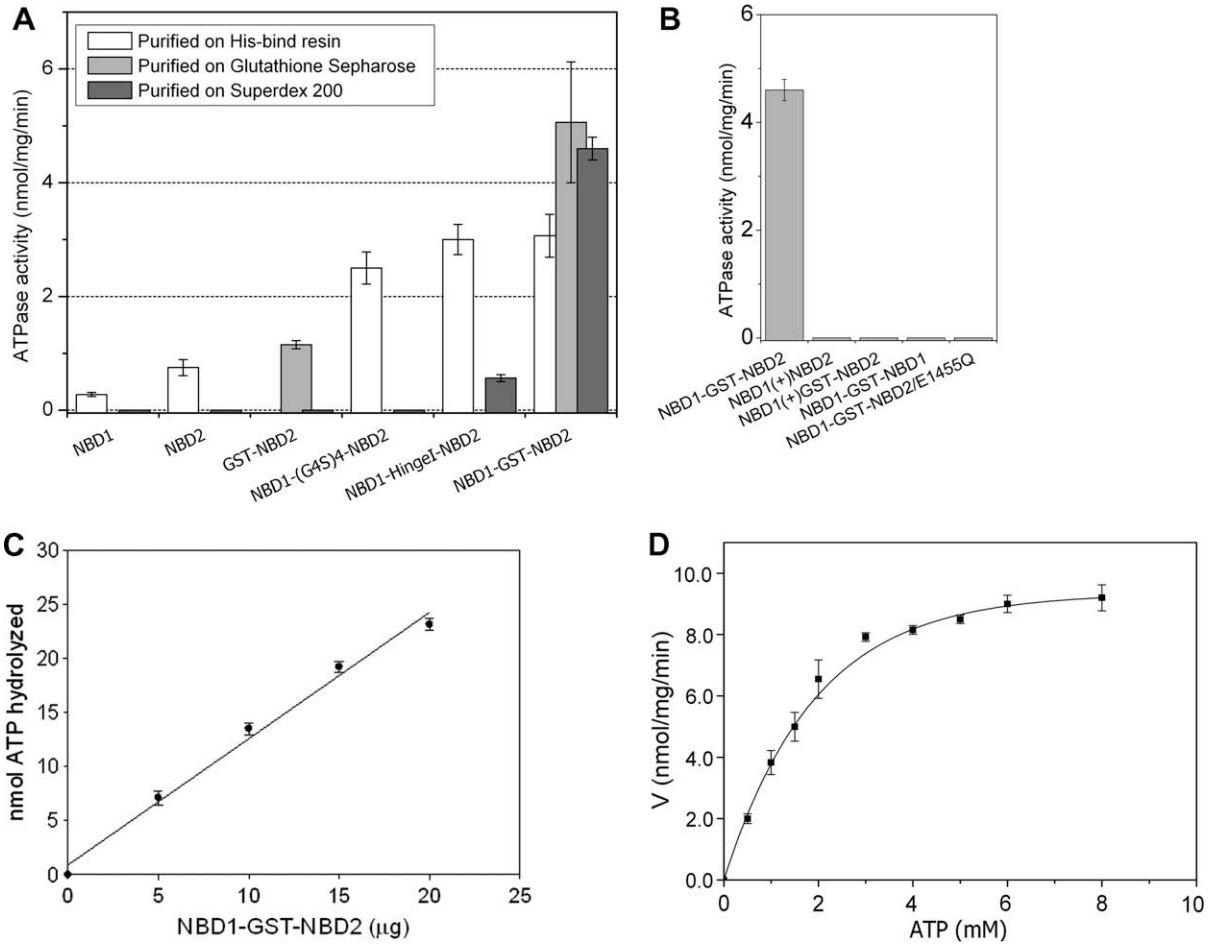

Figure 4. ATPase activity of purified NBD proteins. (A) ATPase activities of 20 μg NBD1, NBD2, GST-NBD2, NBD1-$(G_4S)_4$-NBD2, NBD1-HingeI-NBD2, or NBD1-GST-NBD2 at different purification steps were measured as described in the Materials and methods section. The values are mean ± S.D. of three independent experiments. (B) ATPase activities of the chimeric fusion protein NBD1-GST-NBD2, the NBD1(+)NBD2 mixture, the NBD1(+)GST-NBD2 mixture, NBD1-GST-NBD1, and NBD1-GST-NBD2/E1455Q, all purified from Superdex 200 columns. (C) ATPase activity of varying amounts (5, 10, 15, and 20 μg) of the purified NBD1-GST-NBD2 protein. (D) Effects of increasing ATP concentration on NBD1-GST-NBD2 ATPase activity.

which leads to an increase in the MIANS fluorescence. Excess MIANS was incubated with the purified chimeric fusion proteins for up to 1 h to ensure saturated labeling. Emission spectra monitored at excitation 322 nm indicated a 30–40% increase in fluorescence intensity and a red shift of the emission maximum (λ_{max}) from 426 to 432 nm for NBD1-GST-NBD2 compared to NBD1(+)GST-NBD2 (Fig. 5A). Since both proteins had an equal number of cysteine residues and the same amounts of protein (0.1 μM) were used in the assay, the fluorescence change in both fluorescence intensity and λ_{max} of the emission shift suggested a conformational difference between the two proteins that rendered the cysteines of NBD1-GST-NBD2 were more accessible to the solvent than NBD1(+)GST-NBD2 mixture, consequently increasing its MIANS labeling.

Differences in circular dichroism spectra between NBD1-GST-NBD2 chimeric fusion protein and NBD1(+)GST-NBD2 mixture

The far-UV circular dichroism (CD) spectrum of a protein provides information about its secondary structure and can be used to detect structural rearrangements resulting from conformational changes [19], particularly rearrangements in the α-helical structures. The CD spectra of identical molar concentrations of the NBD1-GST-NBD2 chimeric protein and a NBD1(+)GST-NBD2 mixture were recorded, indicating both were typical highly structured α-helical proteins (Fig. 5B). The spectral differences at 208 and 222 nm and the about 25% increase in ellipticity of the NBD1-GST-NBD2 chimeric protein compared with the NBD1(+)GST-NBD2 mixture suggested a secondary structure difference. The results may show that the higher ATPase activity of the chimeric fusion protein NBD1-GST-NBD2 is related to a conformational properties of the molecule.

Discussion

ATP binding and hydrolysis are key steps that provide necessary conformational rearrangements required for substrate relocation in the MRP1 transport cycle. Since the two NBDs of MRP1 are responsible for this function, it is important to study their interactive role in ATP binding and hydrolysis. Unlike P-gp, the intrinsic ATPase activity of MRP1 is so low that crude membrane extracts are unsuitable for direct study of its enzymatic properties. Instead researchers have utilized methods such as photoaffinity labeling and vanadate trapping to mimic transient states in ATP binding and hydrolysis. For example, Hou and colleagues [14,20,21] investigated the asymmetric roles of the two NBDs of MRP1 in ATP binding and hydrolysis. In addition to these efforts, researchers have also successfully cloned the NBD1 and NBD2 domains, which could be expressed and extracted at high yield and purity, especially compared with NBDs from P-gp. However, none of the two MRP1 NBDs could be shown to possess ATPase activity comparable to that of the intact MRP1, and the mixture of two purified NBDs showed only transient interactions between the domains [9,10]. Similarly, our result also indicated the purified NBD1 and NBD2 had no detectable ATPase activity (Fig. 4A). Attempts to co-extract NBD1 with GST-NBD2 failed as NBD1 could not co-purified with GST-NBD2 on a glutathione sepharose column; in addition, NBD1 also failed to co-precipitate with GST-NBD2 in a GST pull down experiment (data not shown). However, when the two NBDs were linked by specific linker peptides, the chimeric proteins were capable of hydrolyzing ATP at a rate similar to that of the intact MRP1, especially in the case of NBD1-GST-NBD2 chimeric fusion protein. In contrast, a mixture equivalent of NBD1 and GST-NBD2 with molar concentrations and amino acid composition as that of NBD1-GST-NBD2, displayed no detectable ATPase activity.

It has been reported that the two NBDs of MRP1 were not equivalent in ATP hydrolysis, NBD1 mainly serving a regulatory role through its binding to ATP, while NBD2 actually hydrolyzes ATP during the transport cycle of the MRP1 [1]. A NBD1-GST-NBD1 chimeric fusion protein purified by the same strategy as used for NBD1-GST-NBD2 was unable to hydrolyze ATP. In order to identify the properties of the NBD1-GST-NBD2 chimeric fusion protein, we further introduced several mutations in the conserved Walker A and Walker B motifs of its two NBDs (Fig. 4B), targeting reported key residues in both ATPase and substrate transport activitiy of the intact MRP1 [14,22]. Among the NBD1-GST-NBD2 mutants, K684L in Walker A of NBD1, K1333L in Walker A of NBD2, and D1454L/E1455L in Walker B of NBD2 were expressed mainly as inclusion bodies in *E. coli*, and only the E1455Q mutant was expressed in a sufficient quantity of soluble protein to allow activity analysis. The results clearly showed that the NBD1-GST-NBD2/E1455Q mutant was not functional, consistent with a previous report on this null-mutant in the intact MRP1 [22]. These results confirmed our finding that the observed ATPase activity was an intrinsic property of the NBD1-GST-NBD2 chimeric fusion protein rather than the result of contamination.

The sensitivity of an enzyme to a specific inhibitor can be also used to identify its enzymatic properties. Vanadate is an inhibitor of some ATPases by mimicking the phosphate group involved in phosphoryl transfer [23]. Most ABC type ATPases including MRP1 are vanadate-sensitive, the IC_{50} of Na_3VO_4 is about 10 μM for MRP1 [6]. However, the NBD1-GST-NBD2 chimeric fusion protein did not show any significant sensitivity to vanadate, as its activity still remained about 85% of the control even in the presence of

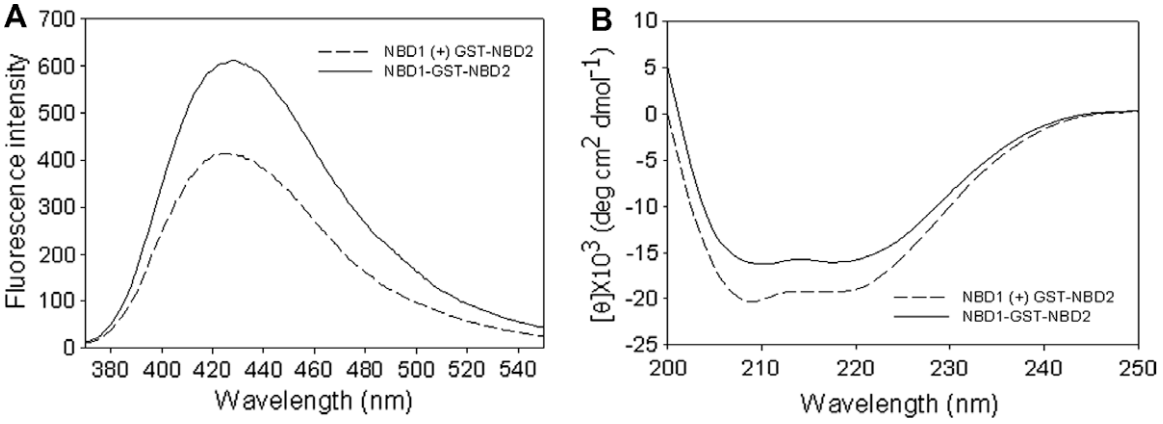

Figure 5. Conformational differences between NBD1-GST-NBD2 chimeric fusion protein and the NBD1(+)GST-NBD2 mixture (A) Emission spectra of MIANS labeled two proteins, (B) Circular dichroism spectra of the two proteins.

100 μM Na_3VO_4 (data not shown). It has been suggested that in the case of intact ABC proteins, vanadate can only mimic phosphate when the amino acids of the ATP binding pocket (formed by the two NBDs) are so arranged as to facilitate the most suitable configuration for ATP binding and hydrolysis [23]. In the NBD1-GST-NBD2 chimeric fusion protein, the ATP binding pocket may differ slightly from that of the intact MRP1, which may prevent the functional mimicking by vanadate. The observation that the fusion protein showed a much lower affinity for ATP than the intact MRP1 further supports this explanation. In further studies, it would be interesting to resolve the 3-D structure of the NBD1-GST-NBD2 chimeric fusion protein and thus obtain more information on the fine structure of interaction between the NBD1 and NBD2 domains.

The method of using purified NBDs to investigate ATPase activity of intact protein have also been employed in studies of other ABC transporters, however, to our knowledge, stable interaction between purified wild type NBDs of eukaryotic ABC transporters has not yet been reported. Several recently resolved crystal structures of NBD-NBD homodimers have been obtained by introducing mutations in the ATP binding site to stabilize the NBD-NBD interaction, with the consequence that they were all nonfunctional [24–26]. Therefore, a reasonable approach could be to add an additional peptide linker between two NBDs to facilitate a direct and stable interaction. Following this idea, to connect NBD1 and NBD2 of MRP1, we designed six different peptide linkers with lengths ranging from 20 to 219 amino acids and expressed the corresponding chimeric fusion protein constructs (Fig. 1). Among these, proteins with short peptides linkers were found to be nonfunctional. The short linkers were either flexible peptides, like $(G_4S)_4$, or helical peptides, like $(EAAAR)_4$. However, these short linkers of 20–40 amino acids may have been too short to provide proper spatial arrangement for the interaction between two NBDs. We therefore tested two longer peptides to link the two NBDs, the 42 amino acids long RLI Hinge I region, and the 219 amino acids long GST protein. These two chimeric proteins were capable of hydrolyzing ATP even when purified on a Superdex 200 gel filtration column (Fig. 4A). This was particularly true for the NBD1-GST-NBD2 chimeric fusion protein, which showed an ATPase activity of 4.6 nmol/mg/min ($6.34 \times 10^{-3}\ s^{-1}$), with V_{max} and K_m values determined as 12.36 nmol/mg/min ($17.0 \times 10^{-3}\ s^{-1}$) and 2.17 mM, respectively. This activity was comparable with that of intact MRP1 (V_{max} = 5–10 nmol/mg/min or 16–32 $\times 10^{-3}\ s^{-1}$,) but the affinity of NBD1-GST-NBD2 for ATP was less than that of the intact MRP1 (K_m = 100–300 μM). It has been clearly demonstrated that the conserved motifs Walker A, stacked aromatic residues, and the Q-loop of one NBD interact with the ABC signature motif of the opposite NBD, to form two ATP binding pocket between two NBDs to bind ATP molecules. This "sandwich dimerization" of two NBDs is a unique feature shared by the ABC type of ATPases, and represents a structure that is finely regulated during the ATP hydrolysis cycle. Isolated NBDs or short linker chimeric fusion proteins appeared unable to provide the proper conformational arrangements required for functional NBD-NBD interaction, whereas a longer linker such as GST might be able to allow an interaction between the two NBDs that facilitated ATP hydrolysis. However, it is also reasonable that because an optimal conformational arrangement of the NBDs may depend on additional interactions with groups in the intact MRP1, the chimeric fusion protein may not entirely recapitulate their functionality in the intact protein, as suggested by the lower affinity for ATP in the chimeric fusion protein. Despite this difference, our results provide a novel approach to the study of ATPase activity of the two NBDs of MRP1, and may also provide further clues to the study of domain-domain interactions in large membrane proteins.

It is widely agreed that the proper conformation of a protein is necessary for its activity. The relationship between the intrinsic ATPase activity and the conformation of NBD1-GST-NBD2 chimeric fusion protein compared to a NBD1(+)GST-NBD2 mixture was further characterized by using MIANS fluorescent labeling and CD spectroscopy. As indicated clearly in Fig. 5, there were significant differences in both the fluorescence and the CD spectra between the chimeric fusion protein NBD1-GST-NBD2 and the mixture NBD1(+)GST-NBD2. Given that the amino acid composition and the molar concentrations of chimeric fusion protein and the mixture were almost exactly the same, the CD and fluorescence spectra suggested differences in the higher order structural organization and in the micro-environment of the cysteine residues, respectively, which might explain the higher ATPase activity of the NBD1-GST- NBD2 chimeric fusion protein.

In summary, our results show that the interaction between NBD1 and NBD2 of the MRP1 mediated by GST linker in a novel chimeric fusion protein produces conformational changes which allows for higher ATPase activity. The results may also shed light on important aspects of the interaction between NBD1 and NBD2 domains and their ATPase activity in the intact MRP1.

Acknowledgments

This work was financially supported by the National Basic Research Program of China (Grants 2004CB720000 and 2006CB911001), Chinese Academy of Sciences (07165111ZX), the MOST 973 Program No. 2009CB930200 and National Natural Science Foundation of China (30370350).

References

[1] X.B. Chang, Cancer and Metastasis Reviews 26 (2007) 15–37.
[2] R.J. Dawson, K.P. Locher, Nature 443 (2006) 180–185.
[3] J. Chen, G. Lu, J. Lin, A.L. Davidson, F.A. Quiocho, Mol. Cell. 12 (2003) 651–661.
[4] K.J. Linton, Physiology (Bethesda) 22 (2007) 122–130.
[5] E. Janas, M. Hofacker, M. Chen, S. Gompf, D.C. van der, R. Tampe, J. Biol. Chem. 278 (2003) 26862–26869.
[6] Q. Mao, E.M. Leslie, R.G. Deeley, S.P. Cole, Biochim. Biophys. Acta 1461 (1999) 69–82.
[7] Q. Mao, R.G. Deeley, S.P. Cole, J. Biol. Chem. 275 (2000) 34166–34172.
[8] M. Ramachandra, S.V. Ambudkar, D. Chen, C.A. Hrycyna, S. Dey, M.M. Gottesman, I. Pastan, Biochemistry 37 (1998) 5010–5019.
[9] O. Ramaen, S. Masscheleyn, F. Duffieux, O. Pamlard, M. Oberkampf, J.Y. Lallemand, V. Stoven, E. Jacquet, Biochem. J. 376 (2003) 749–756.
[10] O. Ramaen, C. Sizun, O. Pamlard, E. Jacquet, J.Y. Lallemand, Biochem. J. 391 (2005) 481–490.
[11] O. Ramaen, N. Leulliot, C. Sizun, N. Ulryck, O. Pamlard, J.Y. Lallemand, H. Tilbeurgh, E. Jacquet, J. Mol. Biol. 359 (2006) 940–949.
[12] A. Karcher, K. Buttner, B. Martens, R.P. Jansen, K.P. Hopfner, Structure 13 (2005) 649–659.
[13] X.B. Chang, Y.X. Hou, J.R. Riordan, J. Biol. Chem. 272 (1997) 30962–30968.
[14] Y. Hou, L. Cui, J.R. Riordan, X. Chang, J. Biol. Chem. 275 (2000) 20280–20287.
[15] C.A. Doige, X. Yu, F.J. Sharom, Biochim. Biophys. Acta 1109 (1992) 149–160.
[16] R. Liu, F.J. Sharom, Biochemistry 35 (1996) 11865–11873.
[17] R. Paulmurugan, S.S. Gambhir, Cancer Res. 65 (2005) 7413–7420.
[18] Z. Huang, Y. Huang, Sci. China C. Life Sci. 47 (2004) 425–433.
[19] N.J. Greenfield, Nat. Protoc. 1 (2006) 2876–2890.
[20] Y.X. Hou, L. Cui, J.R. Riordan, X.B. Chang, J. Biol. Chem. 277 (2002) 5110–5119.
[21] Y.X. Hou, J.R. Riordan, X.B. Chang, J. Biol. Chem. 278 (2003) 3599–3605.
[22] R. Yang, A. McBride, Y.X. Hou, A. Goldberg, X.B. Chang, Biochim. Biophys. Acta 1668 (2005) 248–261.
[23] D.R. Davies, W.G. Hol, FEBS Lett. 577 (2004) 315–321.
[24] P.C. Smith, N. Karpowich, L. Millen, J.E. Moody, J. Rosen, P.J. Thomas, J.F. Hunt, Mol. Cell 10 (2002) 139–149.
[25] J. Zaitseva, S. Jenewein, T. Jumpertz, I.B. Holland, L. Schmitt, EMBO J. 24 (2005) 1901–1910.
[26] E. Procko, I. Ferrin-O'Connell, S.L. Ng, R. Gaudet, Mol. Cell 24 (2006) 51–62.